

Thermal laser separation technology for optimized half-cell module performance

Michael Grimm, 3D-Micromac AG, Chemnitz, Germany

Abstract

Half-cell modules are gaining an increasing market share because of their potential for increasing module power without requiring any changes to cell technology. However, it has emerged that different cell separation technologies can produce similar electrical performances of the half cells, yet lead to an entirely different mechanical behaviour of the cells. An electrical evaluation showed minor electrical power losses for the half cells, leading to an efficiency reduction of less than 1%_{rel}. As regards mechanical behaviour, the mechanical strength at the solar cell and module laminate levels was evaluated for thermal laser separation (TLS) and laser scribing with cleaving (LSC) cutting technologies on multicrystalline silicon Al-BSF solar cells. It was possible to systematically show that mechanical defects found at the cell level could also be seen at the module level. More precisely, the mechanical strength in the case of the LSC batch decreased by 35% at the cell level and 23% at the module level. The TLS process, in contrast, did not have an effect on strength at the cell level or the module laminate level. Additionally, the origin of fracture was found to be at the edge for the laser batch and on the rear-side pads for the full cells and TLS-cut cells.

Introduction

The key characteristics of solar cells for half-cell modules are their electrical performance parameters and their mechanical strength. In recent years, there has been significant progress in limiting the electrical losses due to the cell separation process, so that a significant power gain of around 5% can be achieved for half-cell modules [1–3]. On the other hand, the mechanical strength of solar cells is a key parameter with regard to ensuring high yield during the manufacturing of solar cells and modules [4]. Each critical incident of mechanical damage during solar cell production will affect any subsequent process and application, because it will always be the most critical defect that will lead to failure. Furthermore, a reduction in mechanical cell strength leads to increased breakage rates of cells during operation in the field.

In this paper, a systematic study is presented where damage within the solar cell was investigated through fracture tests of single solar cells and of the module or module laminate

(without frame) incorporating the same cells. Thus, the approach allows the mechanical damage at any stage of the production to be quantified. The mechanical tests were accompanied by the determination of the electrical performance of the half cells in order to ensure that either process yields minimal electrical losses due to cell separation. As a result, it was found that different cell separation processes can lead to similar electrical performance parameters of the half cells, while yielding very different levels of mechanical strength.

Material and methods

In the work reported here, commercially available multicrystalline silicon Al-BSF solar cells with four busbars were investigated. The cells were cut into half, either by thermal laser separation (TLS) [5] or by laser scribing with cleaving (LSC). The TLS process was used on the sunny side of the cells, whereas for the LSC process a laser scribe was used on the back side of the cells and cleaved by applying tensile stress, also to the back side of the cells, because of bending. The module laminates were produced using typical standard materials (full-tempered 4mm glass front; Sky S88 EVA encapsulant; Akalight ECS 675 PPE backsheets; Bruker-Spaleck 1.2mm × 0.2mm Solar Tab interconnector). The cell interconnection was performed using a fully automatic tabber-stringer, and lamination was carried out on industrial equipment with process parameters similar to those for industrial processes.

Electrical characterization

In order to quantify the electrical losses induced by the half-cell processes, 30 full cells from each batch were electrically characterized by measuring their illuminated current–voltage curves. Each batch was then split into five reference cells and 25 cells, which were further separated into half cells. In a second measurement sequence, the five reference cells and the 50 half cells were measured once more. The electrical measurements were taken using the LOANA loss analysis tool by pv-tools GmbH. The current–voltage characterization was performed under standard test conditions, and the most relevant electrical performance parameters were obtained by

“The key characteristics of solar cells for half-cell modules are their electrical performance parameters and their mechanical strength.”

applying a two-diode model to the measured data. As a cross check for measurement uncertainty, the data for the five reference cells from each batch was compared for the two measurement runs.

Mechanical characterization

The mechanical strength was determined by means of four-point bending fracture tests in cell and module laminate configurations (see Fig. 1). In four-point bending tests, the samples are supported by two rolls at the bottom and loaded by two rolls at the top, thus creating a fairly constant stress field between the inner rolls. The solar cell tests were performed on a universal testing machine (ZWICK 005), using a load cell of 500N in accordance with DIN SPEC 91351 [6]. For each test, 50 samples were loaded with the rollers parallel to the busbars in the four-point bending set-up until cell breakage occurred for all three batches: 1) full cell without separation; 2) half cell after LSC; and 3) half cell after TLS. Each batch was divided into two tests, with the sunny side or the back side in tension.

The four-point bending configurations used in this work had an outer span (outer rollers) of 80mm and inner load span (inner rollers) of 40mm; the rollers are made of steel with a diameter of 10mm. For better contact behaviour and reduced friction, PTFE foils were placed between the rollers and the cells. A finite-element model was used to calculate the fracture stresses in the four-point bending experiment, taking account of nonlinearities during the bending test [7]. Fracture stresses were evaluated using the Weibull distribution [8,9]. Furthermore, a reduced mechanical cell model was used to capture just the behaviour of the silicon layer, because the metallization does not have a major influence on the stiffness or bending stresses in the four-point bending test for silicon [10]. The metallization, however, governs the defect structure within the silicon layer. For the evaluation of all cells, considering the effect that size has on strength, the effective area was set to $A_{eff} = 9,116\text{mm}^2$; this has also been used in previous publications [11] and allows meaningful comparisons to be made.

The method for in-laminate strength testing is described in detail in Sander et al. [12]. The experimental set-up represents a four-point bending load. With the use of an electroluminescence (EL) camera (Sensovation coolSamBa HR-830), all the cells between the two load rolls can be inspected during the test. The set-up is mounted on a universal testing machine (Zwick Z400). Deflection of the middle of the test sample is measured by a displacement sensor, and load is measured by a 10kN load cell.

All tests were performed at room temperature. The load was increased in steps of 10N and remained constant for 60 sec while the EL image was taken. The test was continued until all cells

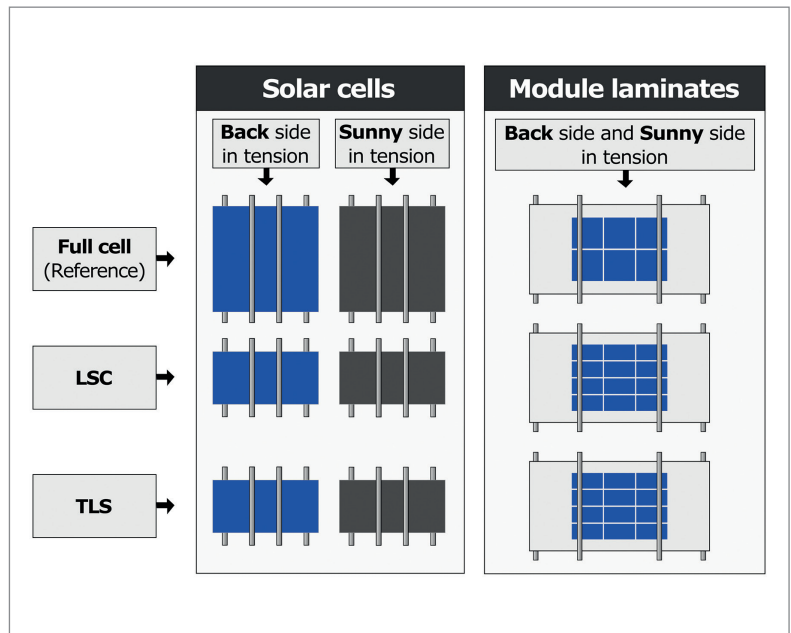


Figure 1. Overview of all the mechanical tests for all the batches (full cell, LSC and TLS), and both configurations (solar cells and module laminates).

were broken or a specified maximum load was reached. As a result of the procedure, load time data and EL images for every load step were available. Crack occurrences can be identified from the load displacement curve when the load decreases abruptly because of a reduction in stiffness of the sample due to a cracked cell. The cracked cell and the fracture origin are identified from the EL images.

In the case of full cells, six module laminates were produced, each incorporating six cells. For the half cells, three module laminates with 12 half cells each were produced for the LSC and TLS batches. In total, it was possible to obtain 36 fracture occurrences for each batch. With regard to the testing of the module laminates, the back and front sides of the cells are in tension. The fracture stresses were calculated by finite-element models and evaluated by means of the Weibull distribution. Some cracks were induced during the lamination process, but these were excluded from the evaluation.

Results

Electrical

The results of the electrical tests reveal minor electrical losses caused by the half-cell processes (see Fig. 2). The power of the half cells is decreased by about 0.5 to 0.8%, which is mainly because of a reduction in the fill factor (see Fig. 2(b)). However, this fill factor reduction cannot be attributed to

“Both cell separation processes lead to fairly high-quality half cells with regard to electrical performance.”

"In the case of the TLS batch, no significant change in mechanical strength could be observed for the sunny side or the back side."

increased recombination, as the pseudo-fill factor (see Fig. 2(c)) remains fairly unaffected by the half-cell process. The reduction in the fill factor can instead be attributed to an increased series resistance during the cell measurements, which can be caused by the different respective contacting schemes used for full and half cells. This contacting-related issue is not expected to occur in a module. Furthermore, it was found that each of the half-cell processes yields similar, moderately loss-less, half cells. Hence, both cell separation processes lead similarly to fairly high-quality half cells with regard to electrical performance.

Mechanical strength of the solar cells

The mechanical strength data of the solar cells are shown in the 90% confidence intervals of the Weibull parameters in Table 1 and Fig. 3. Compared with the full cells, there is a significant 35% reduction in the characteristic fracture stress of the LSC batch on the back side in tension. The scattering of this batch is also significantly decreased. In contrast, on the sunny side in tension, the characteristic fracture stress of the LSC batch is decreased by 10%, compared with the full cells. In the case of the TLS batch, no significant change in mechanical strength could be observed for the sunny side or the back side. It can be assumed, therefore, that no mechanical damage occurs as a result of the TLS process.

Mechanical strength of the module laminates

For the module laminates, the characteristic fracture stress of the LSC batch is decreased by 23%, compared with the full-cell laminate, and the Weibull modulus is increased (Table 2 and Fig. 4). In contrast, the characteristic fracture stress for the TLS batch is increased by 9%, compared with the full-cell laminate, while the Weibull modulus shows no significant difference for all batches.

Cell vs. module: fracture stresses and fracture origin

The fracture stresses of all three batches (full, LSC and TLS) for the solar cell and module laminate configurations are shown in Fig. 5. In general, the fracture stresses of the cell batches are higher than those of the module laminate batches, because of additional soldering and lamination effects and the effect of size on strength due to different evaluated areas. The damage caused by the LSC process can be seen at the cell and module laminate levels, while the fracture stresses dominate in the weaker back side at the module level because of the similar loads on the sunny and back sides in the laminate.

The scattering of fracture stresses for the full-cell batch and the TLS batch are very similar at the solar cell and module laminate levels, which means that in both cases the same defect distributions are addressed. For the LSC batch, however, the scattering is much smaller than that for the other batches at the module laminate level and the cell level. As can be seen from the Weibull parameters (see Fig. 3 and Table 1), the lowest scattering occurs for the LSC cells on the back side, where the laser induces very strong but constant defects.

microCELL™

Highly Productive
Laser Systems
for Half-Cell Cutting



- » Excellent edge quality by TLS-Dicing™
- » Highest throughput in the market:
 - > 5.500 wph on single lane
- » On-the-fly laser processing
- » Contactless single-pass and ablation-free cutting
- » Unbeatable cost-benefit ratio



3D-Micromac AG
Micromachining Excellence
www.3d-micromac.com

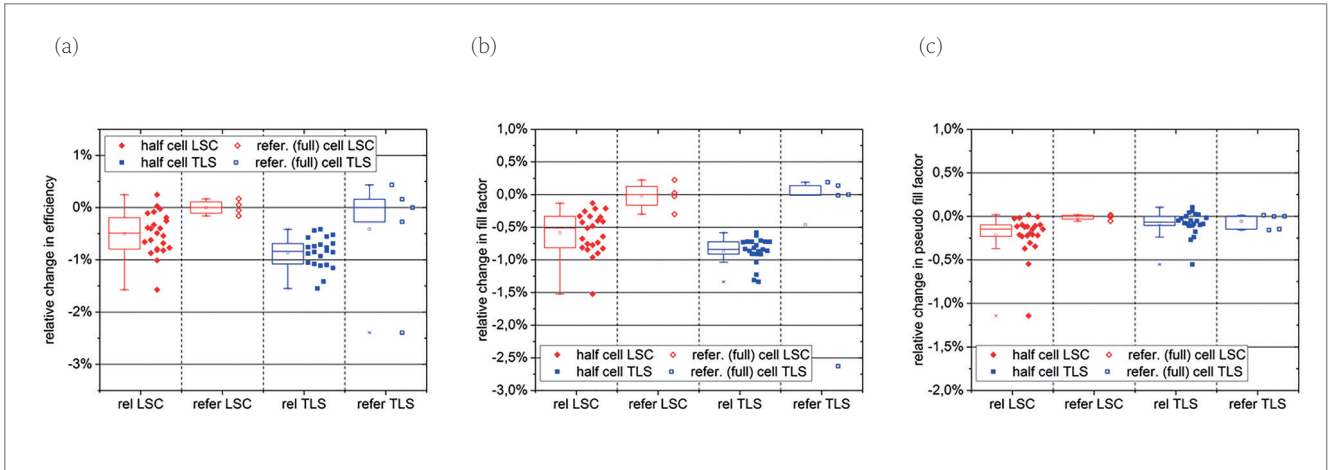


Figure 2. (a) Efficiency losses of half cells compared with full cells. (b) Reduced fill factors of half cells compared with full cells. (c) Pseudo-fill factors of half cells, indicating minor losses compared with full cells.

Batch	Characteristic fracture stress σ_0 [MPa]	Weibull modulus m [-]
Back-full	180.0 (173.8 ... 186.4)	6.9 (5.7 ... 8.3)
Back-LSC	116.1 (114.4 ... 117.8)	17.5 (14.3 ... 21.0)
Back-TLS	176.4 (170.8 ... 182.1)	7.9 (6.6 ... 9.4)
Sunny-full	184.0 (178.3 ... 189.8)	7.8 (6.5 ... 9.3)
Sunny-LSC	166.4 (161.8 ... 171.1)	8.7 (7.2 ... 10.3)
Sunny-TLS	177.5 (172.1 ... 182.7)	8.5 (6.9 ... 10.3)

Table 1. Strength data for the solar cells with 90% confidence intervals (effective area $A_{eff} = 9,116mm^2$).

Examples of the fracture origins found in the laminate fracture tests are shown in Fig. 6. In the case of the full-cell and TLS batches, the fracture origins were mostly found at the back-side pads, whereas for the LSC batch the fracture origins were mostly found at the cutting edge. This result is in good agreement with the strength data, because the TLS batch does not show any damage; thus, the fracture origin is the same as that for the full-cell batch. On the other hand, the LSC batch suffers significant mechanical damage, confirmed by the fracture origins at the laser cutting edges.

Discussion

The two half-cell separation processes examined in this work yield half cells with comparable minor electrical losses due to the cell cutting. However, major differences between the two types of half cell have been observed in terms of their mechanical strength. The damage of the LSC batch on the back side can be explained, because the laser scribe was performed on the back side. Front-side damage, however, can also occur if the laser scribe penetrates to a depth of more than half of the silicon cell thickness. The results at the cell level are in good agreement with the literature [3,13]. Because the half-cell batches are evaluated by taking into account the effect of size on strength, through using the same effective area as the full-cell batches, a quantitative comparison of strength can be made.

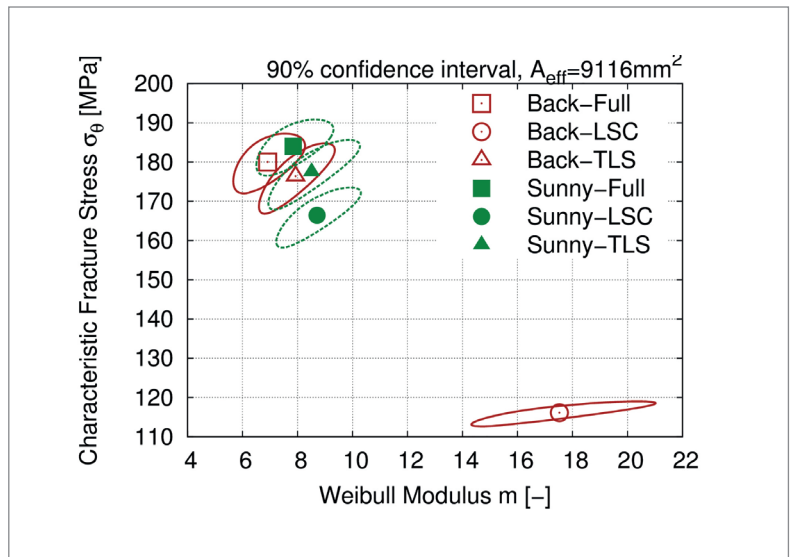


Figure 3. Weibull parameters of the solar cells with 90% confidence intervals.

The strength results for the module laminates are quantitatively lower than the results where only the solar cells were tested; this is because of the effect of size on strength and the additional residual stresses from the soldering and lamination processes. The effect of size on strength means that the probability of finding a critical defect is greater for a larger area than for a smaller one; this is why the strength of a single solar cell has to be less than the strength of six full cells (or twelve half cells) within one module laminate. To evaluate

Batch	Characteristic fracture stress σ_0 [MPa]	Weibull modulus m [-]
Full	102.6 (97.6 ... 107.7)	6.9 (5.4 ... 8.7)
LSC	78.9 (76.0 ... 81.8)	8.7 (7.0 ... 10.6)
TLS	111.5 (105.4 ... 117.6)	6.0 (4.7 ... 7.5)

Table 2. Strength data of the module laminates with 90% confidence interval.

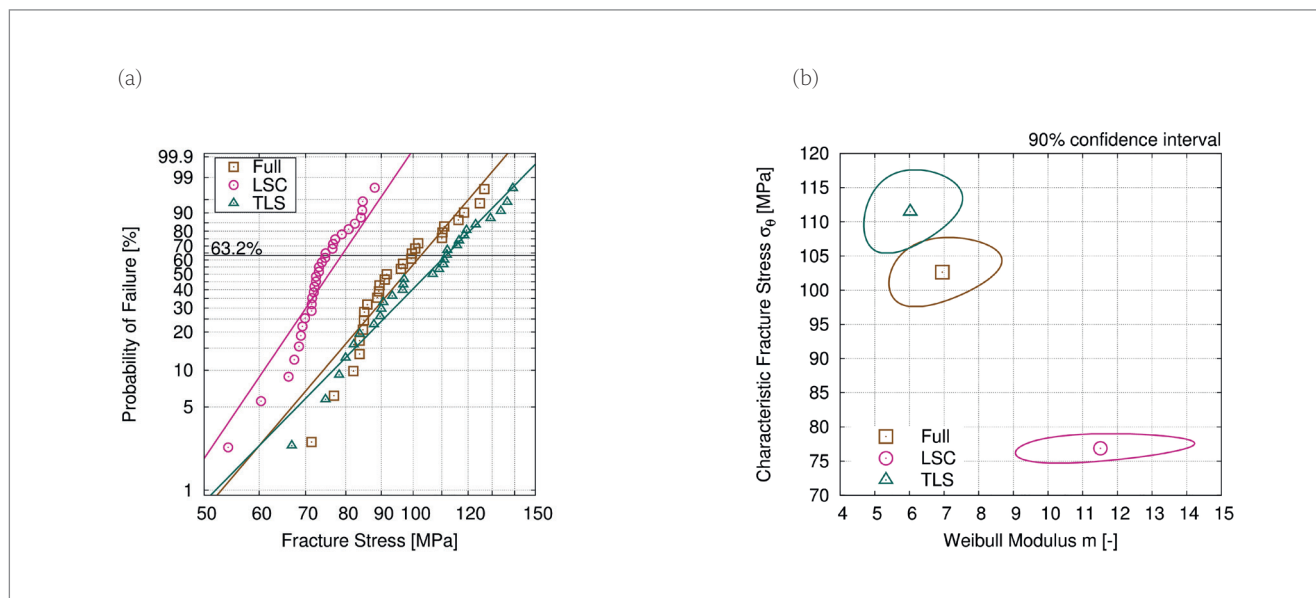


Figure 4. Mechanical strengths of the module laminates: (a) Weibull diagram; (b) Weibull parameters with 90% confidence intervals.

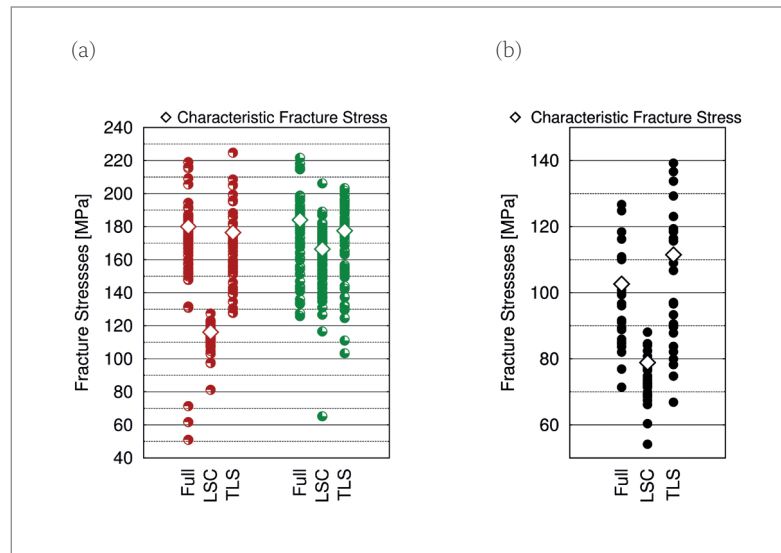


Figure 5. Fracture stresses of full cells and half cells cut by LSC and TLS and tested in a four-point bending set-up: (a) solar cells with $A_{eff} = 9,116 \text{ mm}^2$; (b) module laminates.

this effect, the strength results for the solar cells were applied to the full number and size of the cells in the module laminate configuration ($A_{eff} = 156 \text{ mm} \times 156 \text{ mm} \times 6 = 146,016 \text{ mm}^2$).

Compared with the initial results (see Fig. 7(a)), the transformed cell results (see Fig. 7(b)) differ by approximately 5–30MPa from the module laminate results, which represents the remaining residual stresses arising from the soldering and lamination processes. The largest deviation

occurs for the LSC batch, where the module laminate results still exhibit lower strength, in the range of up to 30MPa, compared with the transformed cell results. This could be explained by the additional loading from the ribbons on the damaged cutting edges; the other two batches, which do not have additional damage at the edges, will not be affected. Note that the effective area of a single cell within the laminate can be much smaller than the full area of the cell as a result of inhomogeneous stress fields of the lamination and soldering processes.

Conclusions

In the work reported in this paper, two solar cell separation processes – namely LSC and TLS – were investigated, with a particular focus on the mechanical defects. The cut solar cells were evaluated at both the cell level and the module laminate level. The first result was that both processes lead to similar half cells from an electrical point of view, while the mechanical properties of the half cells are very different. Second, it was shown that the defects responsible for breakage at the cell level are the same as those at the module laminate level. In particular, it was found that the LSC cut edge of half cells is predominant in the breakage at the cell and module laminate levels. In contrast to this, the TLS process did not show any significant mechanical damage to the cells.

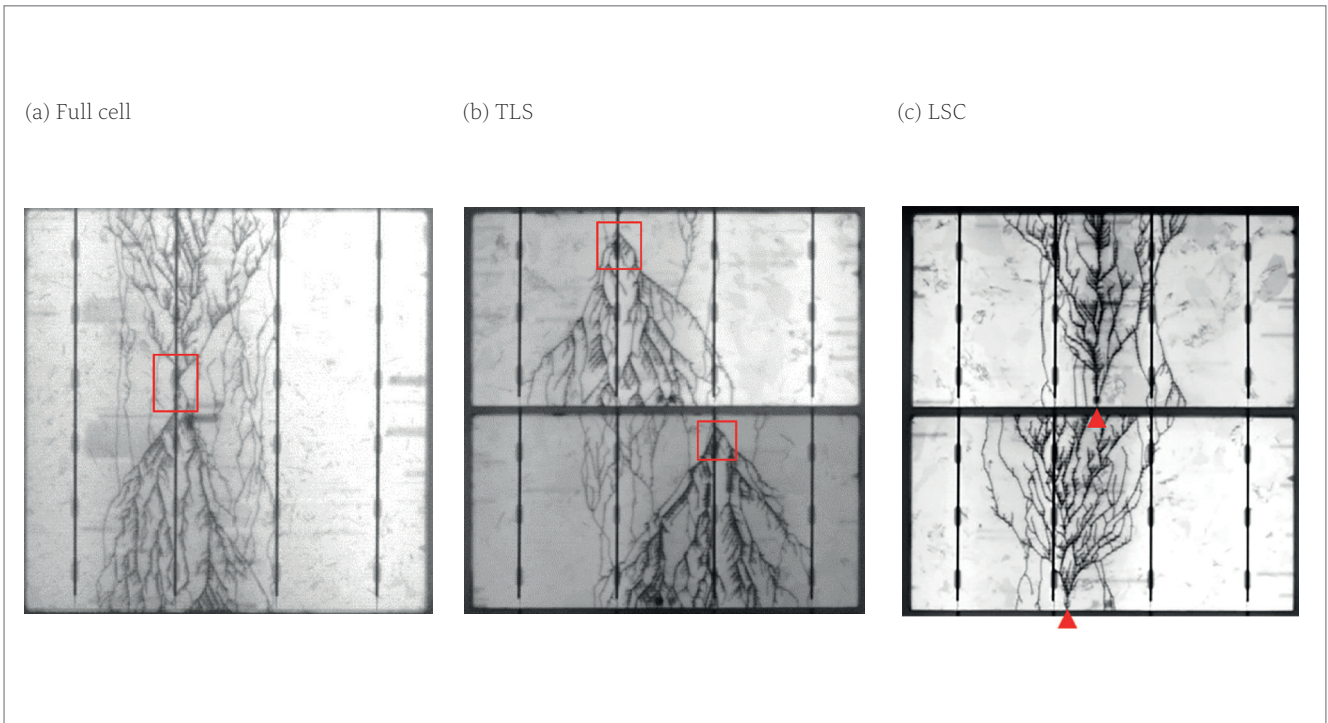


Figure 6. EL images (contrast and brightness adjusted) of broken cells from the module laminate fracture tests with fracture origin at the busbars (red squares) for (a) full cells and (b) TLS, and at the cutting edge (red triangles) for (c) LSC.

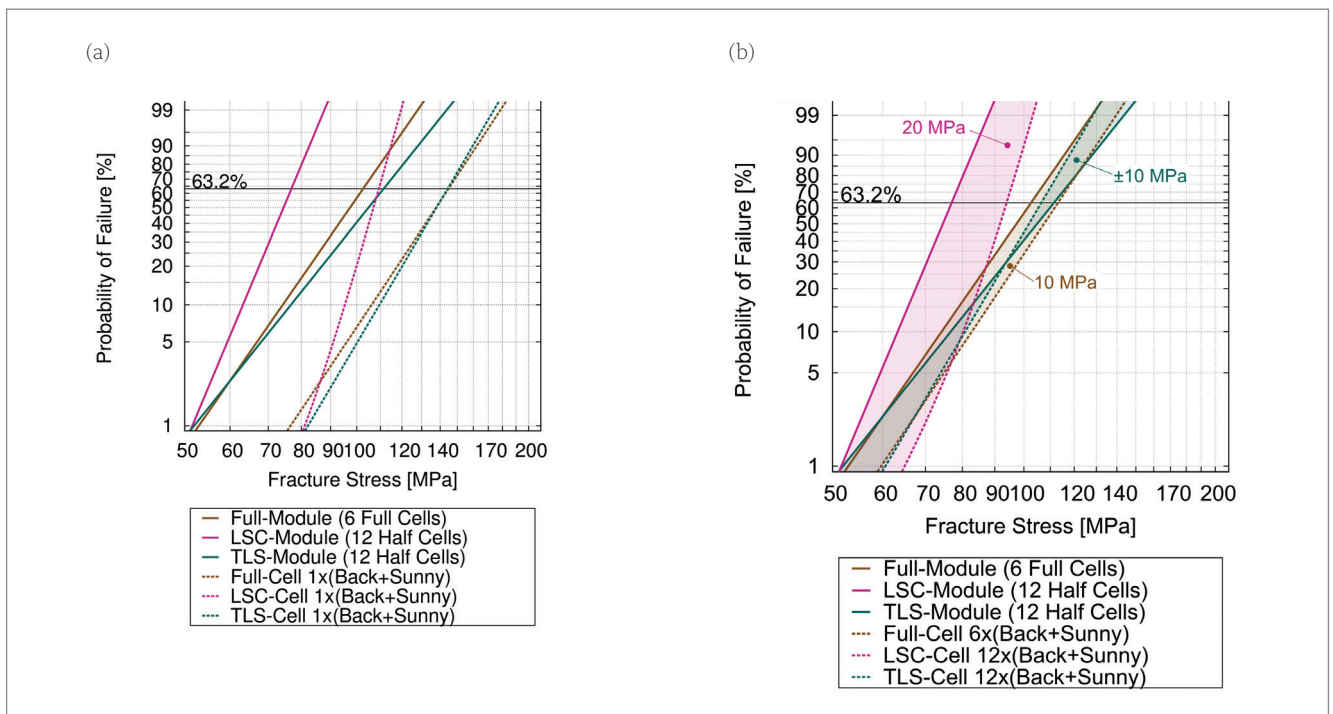


Figure 7. Application of the mechanical cell results to the module laminate configuration: (a) initial data at the module laminate and cell levels (1 full cell/1 half cell); (b) initial data at the module laminate and cell levels evaluated in terms of the size of the module laminate (6 full cells/12 half cells)

In conclusion, the mechanical testing of solar cells gives a fairly good quantitative estimate of the mechanical cell properties in the module laminate. Hence, the testing of solar cells with regard to their mechanical strength does not just characterize the cell and module production in terms of damage and yield; indeed, the testing provides more insights into the reliability of the modules in field conditions. The separation

processes strongly influence cell and module reliability and must be optimized for modules with small breakage rates.

“The LSC batch suffers significant mechanical damage, confirmed by the fracture origins at the laser cutting edges.”

“The mechanical testing of solar cells gives a fairly good quantitative estimate of the mechanical cell properties in the module laminate.”

Outlook

Next-generation modules with further improved performance beyond the half-cell approach are already in development. The process of cutting solar cells into small strips and assembling them by shingling leads to a further reduction in electrical losses and to an enhanced active module area.

For cell cutting, the industrial approach of TLS dicing will be implemented and further optimized. The possibility of achieving excellent edge re-passivation for almost-perfect edges using TLS will be evaluated by means of various techniques, such as H₂ passivation carried out by plasma immersion deposition methods using organic layers. The main efforts will centre on the optimization of laser cutting in order to minimize recombination losses, as well as on demonstrating improved performance and reliability of shingled modules.

Shingling equipment based on electrically conductive adhesive (ECA) printing is in development and will target the assembly of thin (100–160 μm) silicon heterojunction (SHJ) cells at a nominal throughput of 4,000 wph in a dual-lane configuration. This will be realized with a new TLS-dicing module with a bidirectional cutting head to cut cells into quarter-size strips, or smaller, and stack them into cassette bins. Integration kits of TLS dicing heads in third-party equipment will be also available.

Acknowledgements

This work was supported by the German Federal Ministry of Economic Affairs and Energy (BMWi) within the framework of the Solar-TLS research project (Contract No. 032583C). The author would like to thank F. Kaule, M. Pander, M. Turek and S. Schoenfelder from Fraunhofer Center for Silicon Photovoltaics CSP in Halle (Saale), Germany, and E. Hofmueller from Cell Engineering GmbH in Kabelsketal, Germany, for their constant support and encouragement on this research project. He would also like to thank K. Bühler for the fruitful discussions. Work and activities regarding solar cell strips for shingled modules are financially supported through the HighLite project, funded by the EU.

References

- [1] Eiternick, S. et al. 2014, “Loss analysis for laser separated solar cells”, *Energy Procedia*, Vol. 55.
- [2] Guo, S. et al. 2015, “Investigation of the short-circuit current increase for PV modules using halved silicon wafer solar cells”, *Sol. Energy Mater. Sol. Cells*, Vol. 133.
- [3] Eiternick, S. et al. 2015, “High quality half-cell

processing using thermal laser separation”, *Energy Procedia*, Vol. 77.

- [4] Kaule, F., Meyer, S. & Schoenfelder, S. 2017, “Benchmarking mechanical strength data for new solar cell concepts”, *Proc. 33rd EU PVSEC*, Amsterdam, The Netherlands.
- [5] Zuehlke, H.-U. 2009, “Thermal laser separation for wafer dicing”, *Solid State Technol.*, pp. 24–27.
- [6] DIN SPEC 91351, “Strength testing for photovoltaic wafers”.
- [7] Schoenfelder, S. et al. 2011, “Mechanical characterisation and modelling of thin chips”, in *Ultra-thin Chip Technology and Applications*, Burghartz, J., Ed., New York: Springer, pp. 195–218.
- [8] Weibull, W. 1939, *A Statistical Theory of the Strength of Materials*. Stockholm: Generalstabens Litografiska Anstalts Förlag.
- [9] Weibull, W. 1951, “A statistical distribution function of wide applicability”, *J. Appl. Mech.*, pp. 293–297.
- [10] Kaule, F., Wang, W. & Schoenfelder, S. 2014, “Modeling and testing the mechanical strength of solar cells”, *Sol. Energy Mater. Sol. Cells*.
- [11] Kaule, F. et al. 2015, “Comprehensive analysis of strength and reliability of silicon wafers and solar cells regarding their manufacturing processes”, *Photovoltaics International*, 29th edn, pp. 22–29.
- [12] Sander, M. et al. 2013, “Systematic investigation of cracks in encapsulated solar cells after mechanical loading”, *Sol. Energy Mater. Sol. Cells*, Vol. 111, pp. 82–89.
- [13] Röth, J. et al. 2015, “Thermal laser separation (TLS) dicing process study – A new technology for cutting silicon solar cells for high-efficiency half-cell modules”, *Proc. 31st EU PVSEC*, Hamburg, Germany.

About the Author

Michael Grimm received his Diploma in physics from Chemnitz University of Technology, and his Ph.D. in physical chemistry from the University of Wuerzburg in Germany. After a postdoctoral position at University College Dublin, he worked for several years for an equipment supplier in the solar industry, before joining 3D-Micromac in 2013. He has held various positions in the company and currently leads the Department of Technology Management, where he is responsible for technology and IP management, public-funded research projects, and national and international research cooperation.

Enquiries

Mandy Gebhardt
3D-Micromac AG
Technologie-Campus 8
09126 Chemnitz, Germany

Email: Gebhardt@3d-micromac.com